Design of Precoded Waveform With Low PAPR for High Mobility Communication Systems

Yufan Chen, Dongxuan He, Zhiping Lu, Minghao Yuan, and Hua Wang, *Member, IEEE*

***Abstract*— In this letter, the low peak to average power ratio (PAPR) precoded waveform design for high mobility communication systems is studied. Based on the time domain equivalent received signal model, a generalized transceiver framework for precoded waveforms is developed, where the computational complexity of the equalizer can be reduced by utilizing the sparse time-delay (TD) domain channel matrix. Further, a minimum signal to interference plus noise ratio (SINR) maximization precoded waveform scheme is proposed, where the precoder and equalizer are calculated jointly using an alternating optimization algorithm. The proposed precoded waveform also holds low PAPR by constraining the l_n-norm of the precoder matrix. Simulation results demonstrate that the proposed precoded waveform can achieve better performance than existing waveforms in terms of both PAPR and bit error rate (BER).**

***Index Terms*— Doubly selective fading, precoded waveform design, PAPR restriction, alternating optimization.**

I. Introduction

UNDER high mobility communication scenarios, multi-path and Doppler effects usually result in doubly selective fading channels. Conventional multi-carrier waveforms like orthogonal frequency division multiplexing (OFDM) are susceptible to doubly selective fading, and thus suffer from severe bit error rate (BER) performance degradation. Furthermore, the high peak to average power ratio (PAPR) is another demerit of OFDM. Existing studies have proposed schemes based on channel coding [1], [2], and precoding [3], [4], [5], [6] to reduce PAPR. Compared to coding-based approaches, precoding has been regarded as a good solution to improve the overall BER performance under selective fading without redundant information [7].

If channel state information (CSI) is available at the transmitter, CSI based precoding schemes can be implemented, which aim at compensating for the channel impairments at the transmitter. In [8] and [9], the authors proposed precoders for OFDM systems with zero forcing (ZF) and minimum mean square error (MMSE) equalizers to minimize the BER under slow fading channel. The authors of [10] proposed a precoder towards BER minimization for OFDM systems with insufficient cyclic prefix (CP). For fast fading channel, precoding was studied in [11], where the authors proposed an eigenvalue decomposition (EVD) based adaptive precoder for an OFDM system with MMSE frequency domain block-wise equalization, which aims at maximizing the minimum signal to noise ratio (SNR) to improve the BER performance.

Nevertheless, little attention was paid to PAPR restriction in existing studies on CSI based precoded waveforms [8], [9], [10], [11]. Additionally, in the presence of fractional Doppler shifts, the Doppler spreads to all Doppler bins and results in a dense frequency-Doppler domain channel matrix, which increases the complexity of the frequency domain block-wise channel equalizer in [11]. These challenges motivate us to develop a novel transceiver model and design a novel precoding scheme to overcome the shortcomings of the existing schemes.

The contributions of this letter are summarized as:

1) A generalized transceiver framework for time domain precoded waveforms is developed, where existing waveforms can be generated. By utilizing the sparse TD domain channel matrix, the computational complexity of the channel equalizer can be reduced, even with fractional Doppler shifts.
2) Based on the generalized framework, a novel precoded waveform scheme for minimum SINR maximization is proposed. The proposed waveform holds low PAPR by constraining the l_1-norm of the precoder matrix. Simulation results demonstrate that the proposed waveform achieves better PAPR and BER performance than other existing waveforms.

Notations: The superscripts $(\centerdot)^T$, $(\centerdot)^H$ and $(\centerdot)^n$ represent the transpose, conjugate transpose, and nth-power operation, respectively. $\sum(\centerdot)$ is the summation operator. $\delta(\centerdot)$ denotes the Dirac delta function. $\|\centerdot\|_n$ denotes the l_n-norm. The notation $\otimes$ denotes the Kronecker product. The normalized N-point discrete fourier transform (DFT) and inverse DFT (IDFT) matrices are denoted by $\mathbf{F}_N$ and $\mathbf{F}_N^H$, respectively.

II. Precoded Waveform Framework Using Time Domain Equivalent Signal Model

In this section, a generalized precoded waveform framework is developed based on the time domain signal model. Existing waveforms can be generated from this framework.

A. Time Domain Equivalent Signal Model

Considering a doubly selective fading channel, the continuous-time domain received signal is given by [12]

$$r(t) = \int\int h(\tau,\nu)s(t-\tau)e^{j2\pi\nu(t-\tau)}d\tau d\nu + v(t), \quad (1)$$

Manuscript received 6 May 2024; revised 17 June 2024; accepted 15 July 2024. Date of publication 19 July 2024; date of current version 12 September 2024. This work was supported in part by State Key Laboratory of Wireless Mobile Communications, China Academy of Telecommunications Technology (CATT), in part by the BIT Research and Innovation Promoting Project (Grant No.2023YCXY029), in part by the National Key Research and Development Program of China under Grant 2020YFB1807900, also in part by the National Natural Science Foundation of China under Grant 62101306. The associate editor coordinating the review of this letter and approving it for publication was J. Guerreiro. *(Corresponding authors: Dongxuan He; Hua Wang.)*

Yufan Chen, Dongxuan He, Minghao Yuan, and Hua Wang are with the School of Information and Electronics, Beijing Institute of Technology, Beijing 100081, China (e-mail: 3120185428@bit.edu.cn; dongxuan_he@bit.edu.cn; minghaoyuan@bit.edu.cn; wanghua@bit.edu.cn).

Zhiping Lu is with the School of Information and Communication Engineering, Beijing University of Posts and Telecommunications, Beijing 100876, China (e-mail: luzp@cict.com).

Digital Object Identifier 10.1109/LCOMM.2024.3430949

where $s(t)$ is the continuous-time domain transmitted signal, $v(t)$ is the additive white Gaussian noise, $h(\tau,\nu)$ is the delay-Doppler channel response, given by

$$h(\tau,\nu)=\sum_{i=1}^{P}h_i\delta(\tau-\tau_i)\delta(\nu-\nu_i), \tag{2}$$

where P is the number of paths, h_i, τ_i, and ν_i are the gain, delay, and Doppler shift of the i-th path, respectively.

Considering a block with N_{fft} subcarriers and N symbols, where the subcarrier bandwidth and symbol duration are denoted as Δf and $T=\frac{1}{\Delta f}$ respectively. The normalized delay and Doppler of the i-th path are given by

$$l_i=\tau_i N_{fft}\Delta f, k_i=\nu_i NT. \tag{3}$$

The sampling rate $f_s=N_{fft}\Delta f$ is set sufficient to approximate the path delays to the nearest sampling points in typical wide-band systems [13]. Therefore we do not need to consider non-integer l_i values. However integer k_i is not guaranteed since the duration $NT\ll 1s$ in typical systems. The discrete-time signal after CP removal is given by

$$r(n)=\sum_{i=1}^{P}h_i e^{j2\pi\frac{k_i(n-l_i)}{N_{fft}N}}s([n-l_i]_{N_{fft}N})+v(n), \tag{4}$$

where $0\le n\le N_{fft}N-1$. After serial-to-parallel conversion, the received signal can be denoted in vector form as

$$\mathbf{r}=\mathbf{H}\mathbf{s}+\mathbf{v}, \tag{5}$$

where $\mathbf{v}\in\mathbb{C}^{N_{fft}N\times 1}$ is the noise vector and $\mathbf{H}\in\mathbb{C}^{N_{fft}N\times N_{fft}N}$ is the TD domain channel matrix, given by

$$\mathbf{H}=\sum_{i=1}^{P}h_i\mathbf{\Pi}^{l_i}\mathbf{\Delta}^{(k_i)}, \tag{6}$$

where $\mathbf{\Pi}=circ\{[0,1,0,\cdots,0]^T_{N_{fft}\times N}\}$ is a permutation matrix and

$$\mathbf{\Delta}^{(k_i)}=diag\left(e^{\frac{j2\pi k_i(0)}{N_{fft}N}},e^{\frac{j2\pi k_i(1)}{N_{fft}N}},\cdots,e^{\frac{j2\pi k_i\left(N_{fft}N-1\right)}{N_{fft}N}}\right).$$

It can be observed from (6) that the number of nonzero elements of $\mathbf{H}$ is determined by $\sum_{i=1}^{P}\mathbf{\Pi}^{l_i}$. In most practical mobile channels, the number of paths $P\ll N_{fft}N$, resulting in a sparse structure of $\mathbf{H}$. Note that for a short frame with fractional normalized Doppler shifts, the sparsity of TD domain channel in (6) still holds. Therefore, employing a TD domain channel equalizer can lead to a substantial reduction in computational complexity compared to using a frequency domain block-wise equalizer with a dense equivalent channel matrix. For example, the complexity of MMSE channel equalizer is reduced from $\mathcal{O}((N_{fft}N)^3)$ to $\mathcal{O}(P^2(N_{fft}N))$.

B. Generalized Precoded Waveform Framework

By utilizing the equivalent signal model in (5), a generalized framework of time domain precoded waveforms is developed, as shown in Fig.1, where S/P and P/S stand for serial-to-parallel and parallel-to-serial conversions, respectively. The parallel signal after precoding is denoted in vector form as

$$\mathbf{s}=\mathbf{U}\mathbf{x}, \tag{7}$$

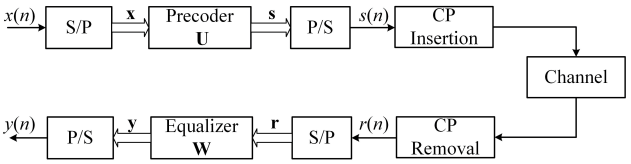

Fig. 1. Transceiver framework for precoded waveform.

where $\mathbf{U}\in\mathbb{C}^{N_{fft}N\times MN}$ is the generalized precoder matrix, which performs precoding and upsampling to N consecutive symbols of length M. After equalization using the equalizer $\mathbf{W}\in\mathbb{C}^{MN\times N_{fft}N}$, the recieved signal is denoted as

$$\mathbf{y}=\mathbf{W}\mathbf{r}=\mathbf{W}\mathbf{H}\mathbf{U}\mathbf{x}+\mathbf{W}\mathbf{v}. \tag{8}$$

Existing waveforms like OFDM and discrete fourier transform spread OFDM (DFT-s-OFDM) can be treated as precoded waveforms and generated using such framework, where $N=1$ and $\mathbf{x}\in\mathbb{C}^{M\times 1}$, the precoder matrices are given by

$$\mathbf{U_{OFDM}}=\mathbf{F}^H_{N_{fft}}\mathbf{Z}, \tag{9}$$

$$\mathbf{U_{DFT-s-OFDM}}=\mathbf{F}^H_{N_{fft}}\mathbf{Z}\mathbf{F}_M, \tag{10}$$

respectively, where $\mathbf{Z}\in\mathbb{C}^{N_{fft}\times M}$ is the zero padding matrix that maps M modulated symbols into N_{fft} subcarriers.

The orthogonal time frequency space (OTFS) waveform has been proposed to improve time and frequency diversity gain in fast fading channels [14]. OTFS can also be generated in the form of (7), where the transmitted and precoded symbols are vectorized as $\mathbf{x}\in\mathbb{C}^{MN\times 1}$ and $\mathbf{s}\in\mathbb{C}^{N_{fft}N\times 1}$ respectively. The precoder matrix $\mathbf{U_{OTFS}}\in\mathbb{C}^{N_{fft}N\times MN}$ is derived as

$$\begin{aligned}\mathbf{U_{OTFS}}&=(\mathbf{F}^H_N\otimes\mathbf{I}_{N_{fft}})(\mathbf{I}_N\otimes\mathbf{F}^H_{N_{fft}}\mathbf{Z}\mathbf{F}_M)\\&=\mathbf{F}^H_N\otimes\mathbf{F}^H_{N_{fft}}\mathbf{Z}\mathbf{F}_M.\end{aligned} \tag{11}$$

If the TD domain channel $\mathbf{H}$ is perfectly known at the transmitter, CSI based precoding can be implemented. The adaptive EVD precoding [11] is reformulated based on the proposed framework as

$$\mathbf{U_{EVD}}=\mathbf{Q}\mathbf{F}^H_{N_{fft}}\mathbf{Z}\mathbf{F}_M, \tag{12}$$

where $\mathbf{Q}$ is obtained by EVD of $\mathbf{H}^H\mathbf{H}$, as

$$\mathbf{H}^H\mathbf{H}=\mathbf{Q}\mathbf{\Lambda}\mathbf{Q}^H. \tag{13}$$

III. Low PAPR Precoded Waveform Scheme

Although the adaptive EVD precoding scheme can achieve lower BER than non-CSI based precoding, the PAPR of the precoded waveform is as high as that of OFDM, which means it is susceptible to nonlinear distortions. This motivates us to design a novel precoding scheme that can improve the error performance while holding low PAPR.

Since the equivalent transmission matrix $\mathbf{T}=\mathbf{W}\mathbf{H}\mathbf{U}$ that achieves minimum BER may not be strictly diagonal, there may be residual interference between received symbols. Minimal BER can be obtained by maximizing the minimum signal to interference plus noise ratio (SINR) of the received symbols. The SINR of the m-th data symbol is calculated as

$$\mathbf{SINR}_m=\frac{\left|[\mathbf{WHU}]_{m,m}\right|^2}{\sigma_v^2+\sum_{i\neq m}\left|[\mathbf{WHU}]_{m,i}\right|^2}, \tag{14}$$

where σ_v^2 is the noise power. Our purpose is to design the precoder $\mathbf{U}$ and the equalizer $\mathbf{W}$ to maximize the minimum SINR, subject to the average power constraints and frequency domain zero index constraints of $\mathbf{U}$, as well as the power normalization constraint of $\mathbf{W}$. The problem is formulated as

$$\begin{aligned} \underset{\mathbf{U},\mathbf{W}}{\text{maximize}} \quad & \min_{m=1,\ldots,M} \mathbf{SINR}_m \\ \text{s.t.} \quad & \|\mathbf{U}\|_2 \le 1, \\ & \|\mathbf{W}\|_2 = 1, \\ & [\mathbf{F}_{N_{fft}}\mathbf{U}]_z = 0, \quad z \in \mathbf{ZI}, \end{aligned} \tag{15}$$

where $\mathbf{ZI}$ contains the index of zero rows of $\mathbf{Z}$, since only M rows of the equivalent subcarrier mapping matrix $\mathbf{F}_{N_{fft}}\mathbf{U}$ are set nonzero to maintain the same frequency occupancy with OFDM. Problem (15) is not convex in variables $\mathbf{U}$ and $\mathbf{W}$. To this end, an alternating optimization method is proposed in this section to jointly calculate matrices $\mathbf{U}$ and $\mathbf{W}$.

A. Precoder& Equalizer Design With the Other Given

For the precoder $\mathbf{U}$ design with given $\mathbf{W}$, besides the maximization of minimum SINR, the construction of $\mathbf{U}$ for PAPR restriction is additionally considered. From (9), (10), and (11), it can be found that the precoder matrix of DFT-s-OFDM has sparse rows when compared to OFDM and OTFS, i.e. most of the elements in each row approach 0. This means in DFT-s-OFDM, only a few input symbols in $\mathbf{x}$ are superposed on each time domain sample of $\mathbf{Ux}$. This property motivates us to design $\mathbf{U}$ with sparse rows. In this way, the input symbols are not constructively superposed. Only very few input symbols contribute to each output sample and the single carrier characteristics can be preserved [3], [4]. This will lead to a reduction of the peak amplitude of the output sample, which further results in a reduction of PAPR. Strict sparsity of a matrix is measured by l_0-norm. However, optimization on l_0-norm is an NP-hard problem. As an alternative, one can use l_1-norm as a convex relaxation of l_0-norm and similar sparse solutions can be obtained [15].

Typically one cannot find a $\mathbf{U}$ that maximizes the minimum SINR while minimizing the l_1-norm as well. Alternatively, we consider maximizing the minimal SINR subject to a precoder matrix l_1-norm constraint. Therefore (15) is reformulated as:

$$\mathcal{S}(\mathcal{A}_O) = \begin{cases} \underset{\mathbf{U}}{\text{maximize}} & \min_{m=1,\ldots,M} \mathbf{SINR}_m \\ \text{s.t.} & \|\mathbf{U}\|_1 \le \mathcal{A}_O, \\ & \|\mathbf{U}\|_2 \le 1, \\ & [\mathbf{F}_{N_{fft}}\mathbf{U}]_z = 0, z \in \mathbf{ZI}. \end{cases} \tag{16}$$

In our system, the problem (16) is not solved directly, since the optimal constraint $\mathcal{A}_O$ is initially unknown. To this end, another strategy which minimizes the l_1-norm of $\mathbf{U}$ given the required minimal SINR constraint γ_O is proposed, which is formulated as follows:

$$\mathcal{A}(\gamma_O) = \begin{cases} \underset{\mathbf{U}}{\text{minimize}} & \|\mathbf{U}\|_1 \\ \text{s.t.} & \min_{m=1,\ldots,M} \mathbf{SINR}_m \ge \gamma_O, \\ & \|\mathbf{U}\|_2 \le 1, \\ & [\mathbf{F}_{N_{fft}}\mathbf{U}]_z = 0, z \in \mathbf{ZI}. \end{cases} \tag{17}$$

According to [16], the necessary condition for (17) to be solveable is

$$\gamma_O \le \left(\frac{\sigma_v^2}{E\left(|\mathbf{H}(m,n)|^2\right)} + \frac{M}{rank\left(\mathbf{WH}\right)} - 1 \right)^{-1}.$$

If $\mathcal{A}(\gamma_O)$ is solvable, we have the following theorem:

Theorem 1: The l_1-norm minimization problem $\mathcal{A}(\gamma_O)$ is the dual problem of $\mathcal{S}(\mathcal{A}_O)$ and therefore

$$\mathcal{S}(\mathcal{A}(\gamma_O)) = \gamma_O. \tag{18}$$

In addition, the optimal solution is strictly monotonic increasing in argument γ_O:

$$\mathcal{A}(\gamma_O) > \mathcal{A}(\widetilde{\gamma}_O), \forall \gamma_O > \widetilde{\gamma}_O. \tag{19}$$

Proof: First, we prove (18). Assuming that $\mathbf{U}$ and $\mathcal{A}$ are the optimal argument and objective value of $\mathcal{A}(\gamma_O)$, respectively, while $\widetilde{\mathbf{U}}$ and $\widetilde{\gamma}_O \neq \gamma_O$ are the optimal argument and objective value of $\mathcal{S}(\mathcal{A}_O)$, respectively. If $\widetilde{\gamma}_O < \gamma_O$, this contradicts with the optimality of $\widetilde{\mathbf{U}}$ and $\widetilde{\gamma}_O$ for $\mathcal{S}(\mathcal{A}_O)$, since $\mathbf{U}$ is also feasible for it however provides a larger objective value γ_O. Otherwise, if $\widetilde{\gamma}_O > \gamma_O$, then this is a contradiction for the optimality of $\mathbf{U}$ and $\mathcal{A}$ for $\mathcal{A}(\gamma_O)$, since we can always find $0 < c < 1$ such that $c\widetilde{\mathbf{U}}$ is also feasible for $\mathcal{A}(\gamma_O)$ however provides an objective value no larger than $c\mathcal{A}$.

Next, we prove (19). Assuming that $\mathbf{U}$ and $\mathcal{A}$ are the optimal argument and objective value of $\mathcal{A}(\gamma_O)$, $\widetilde{\mathbf{U}}$ and $\widetilde{\mathcal{A}} \ge \mathcal{A}$ are the optimal argument and objective value of $\mathcal{A}(\widetilde{\gamma}_O)$ with $\widetilde{\gamma}_O < \gamma_O$. However there always exists $0 < c < 1$ such that $c\mathbf{U}$ is also feasible for $\mathcal{A}(\widetilde{\gamma}_O)$ with an objective value $c\mathcal{A} < \mathcal{A} \le \widetilde{\mathcal{A}}$, which is a contradiction for the optimality of $\widetilde{\mathbf{U}}$ and $\widetilde{\mathcal{A}}$ for $\mathcal{A}(\widetilde{\gamma}_O)$. ■

Using Theorem 1, we can solve $\mathcal{S}(\mathcal{A}(\gamma_O))$ by solving $\mathcal{A}(\gamma_O)$ for different γ_O values. The inversion property guarantees that the feasible γ_O and optimal argument $\mathbf{U}$ for $\mathcal{A}(\gamma_O)$ are optimal for $\mathcal{S}(\mathcal{A}(\gamma_O))$. It is further noticed that $\mathcal{A}(\gamma_O)$ is unsolvable when γ_O is very large. Thus the maximum minimal $\mathbf{SINR}_m$ is found by finding the maximum feasible γ_O for $\mathcal{A}(\gamma_O)$, which can be achieved through a bisection search between a range of γ_Os. This procedure has been detailed in Algorithm 1. Note that the objective function of $\mathcal{A}(\gamma_O)$ is convex and the constraints have the form of second-order cone. Thus it is formulated as a second-order cone program (SOCP), which can be solved efficiently using the CVX toolbox [17].

For the design of equalizer $\mathbf{W}$ with given $\mathbf{U}$, (15) is reformulated as

$$\begin{aligned} \underset{\mathbf{W}}{\text{maximize}} \quad & \min_{m=1,\ldots,M} \mathbf{SINR}_m \\ \text{s.t.} \quad & \|\mathbf{W}\|_2 = 1. \end{aligned} \tag{20}$$

The optimal solution for (20) is achieved by using an MMSE equalizer, which is calculated as

$$\mathbf{W} = \widehat{\mathbf{W}}/\|\widehat{\mathbf{W}}\|_2, \tag{21}$$

where

$$\widehat{\mathbf{W}} = \mathbf{U}^H\mathbf{H}^H\left(\mathbf{HUU}^H\mathbf{H}^H + \sigma_v^2\right)^{-1}. \tag{22}$$

[1]Smaller ϵ_1 leads to higher minimum SINR of the precoded waveform, however requires higher search times. The search accuracy is set as $\epsilon_1 = 10^{-3}$ to make a tradeoff between performance and complexity.

Algorithm 1 Precoder Design With Given Equalizer

Input: TD domain channel $\mathbf{H}$, noise power σ_v^2, minimum $\mathbf{SINR}$ search accuracy ϵ_1,[1] equalizer matrix $\mathbf{W}$.

Output: precoder matrix $\mathbf{U}$, minimum SINR γ_O.

1: Initialize the search range of $\mathbf{SINR}$, the upper bound is set as $\gamma_{\max} = 2\left(\frac{\sigma_v^2}{E\left(|\mathbf{H}(m,n)|^2\right)} + \frac{M}{rank(\mathbf{WH})} - 1\right)^{-1}$, the lower bound is set as $\gamma_{\min} = 0$ for the first iteration, otherwise set as $\gamma_{\min} = \gamma_O^{(j-1)}$.
2: Set number of search times counter $i = 1$.
3: **while** $\gamma_{max} - \gamma_{min} > \epsilon_1$ **do**
4: Set $\gamma_O = (\gamma_{\max} + \gamma_{\min})/2$.
5: Solve problem $\mathcal{A}(\gamma_O)$.
6: **if** problem $\mathcal{A}(\gamma_O)$ is solveable, **then**
7: Set $\gamma_{\min} = \gamma_O$.
8: **else**
9: Set $\gamma_{\max} = \gamma_O$, $\mathbf{U}^{(i)} = \mathbf{U}^{(i-1)}$.
10: **end if**
11: Set $i = i + 1$.
12: **end while**
13: Set outputs $\mathbf{U} = \mathbf{U}^{(i)}$, γ_O.

B. Alternating Optimization Algorithm

An alternating optimization scheme is proposed to optimize $\mathbf{U}$ and $\mathbf{W}$ jointly, which is detailed in Algorithm 2. We have the following proposition for the convergence of Algorithm 2:

Algorithm 2 Joint Optimization of Precoder and Equalizer

Input: TD domain channel $\mathbf{H}$, noise power σ_v^2, maximum minimal $\mathbf{SINR}$ search accuracy ϵ_2.

Output: precoder matrix $\mathbf{U}$, equalizer matrix $\mathbf{W}$.

1: Initialize $\mathbf{U}^{(0)}$ that satisfies average power constraint $\left\|\mathbf{U}^{(0)}\right\|_2 \le 1$, minimal SINR $\gamma_O^{(0)} = 0$.
2: Set number of iterations counter $j = 1$.
3: **while** $\gamma_O^{(j)} - \gamma_O^{(j-1)} > \epsilon_2$ **do**
4: Calculate $\mathbf{W}^{(j)}$ using (21) and (22), where $\mathbf{U} = \mathbf{U}^{(j-1)}$.
5: Set $\mathbf{W} = \mathbf{W}^{(j)}$ and calculate the precoder $\mathbf{U}^{(j)}$ and minimum SINR $\gamma_O^{(j)}$ using Algorithm 1.
6: Set $j = j + 1$.
7: **end while**
8: Set outputs $\mathbf{U} = \mathbf{U}^{(j)}$, $\mathbf{W} = \mathbf{W}^{(j)}$.

Proposition 1: Algorithm 2 converges to a local maximum point of the minimum $\mathbf{SINR}_m$.

Proof: Let us denote the objective minimum $\mathbf{SINR}_m$ in (15) by $\mathcal{S}(\mathbf{U}, \mathbf{W})$, from Algorithm 2, we have

$$\mathbf{W}^{(j)} = \arg\max_{\mathbf{W}} \mathcal{S}\left(\mathbf{U}^{(j-1)}, \mathbf{W}\right), \tag{23}$$

therefore

$$\mathcal{S}\left(\mathbf{U}^{(j-1)}, \mathbf{W}^{(j)}\right) \ge \mathcal{S}\left(\mathbf{U}^{(j-1)}, \mathbf{W}\right), \forall \|\mathbf{W}\|_2 = 1, \tag{24}$$

then we have

$$\mathcal{S}\left(\mathbf{U}^{(j-1)}, \mathbf{W}^{(j)}\right) \ge \mathcal{S}\left(\mathbf{U}^{(j-1)}, \mathbf{W}^{(j-1)}\right). \tag{25}$$

TABLE I
SIMULATION PARAMETERS FOR DIFFERENT WAVEFORMS

Parameters	Values
Carrier frequency	6 GHz
Maximum speed	1000 km/h
Maximum Doppler shift	5.54 kHz
Subcarrier spacing Δf	30kHz (for other waveforms) 120kHz (for OTFS)
Number of symbols N	1 (for other waveforms) 4 (for OTFS)
Symbol length M	48 (for other waveforms) 12 (for OTFS)
FFT length N_{fft}	64 (for other waveforms) 16 (for OTFS)
Modulation	QPSK
Channel fading model	TDL-A [20]
Desired delay spread $DS_{desired}$	363ns
Maximum normalized delay l_P	7
Maximum normalized Doppler shift k_P	0.2

Also, we note that

$$\mathbf{U}^{(j)} = \arg\max_{\mathbf{U}} \mathcal{S}\left(\mathbf{U}, \mathbf{W}^{(j)}\right), \tag{26}$$

and therefore

$$\mathcal{S}\left(\mathbf{U}^{(j)}, \mathbf{W}^{(j)}\right) \ge \mathcal{S}\left(\mathbf{U}, \mathbf{W}^{(j)}\right), \forall \mathbf{U} \in \mathcal{M}^{(j)}, \tag{27}$$

where $\mathcal{U}^{(j)}$ denotes the intersection of constraints of $\mathbf{U}$. Note that $\mathcal{U}^{(j-1)} \subseteq \mathcal{U}^{(j)}$ and thus

$$\mathcal{S}\left(\mathbf{U}^{(j)}, \mathbf{W}^{(j)}\right) \ge \mathcal{S}\left(\mathbf{U}^{(j-1)}, \mathbf{W}^{(j)}\right). \tag{28}$$

In conclusion of (25) and (28), we obtain

$$\mathcal{S}\left(\mathbf{U}^{(j)}, \mathbf{W}^{(j)}\right) \ge \mathcal{S}\left(\mathbf{U}^{(j-1)}, \mathbf{W}^{(j-1)}\right). \tag{29}$$

Therefore, the objective function increases at each iteration and eventually converges to a local maximum point. ■

The computational complexity of the precoder matrix is dominated by iteratively solving the SOCP problem $\mathcal{A}(\gamma_O)$ in Algorithm 1, of which the worst-case is $\mathcal{O}\left((N_{fft}M)^{3.5}\log 2\left(1/\epsilon_1\right)\right)$ using the interior point method [18]. Further note that the channel path gains, delays, and Dopplers are almost constant during a coherence period, which is in the order of tens of milliseconds [19]. During one coherence period, the precoder matrix is updated once and applied to all symbols. With given precoder and equalizer matrices, the complexity of precoding and equalizing for each symbol block are both $\mathcal{O}(N_{fft}M)$.

IV. SIMULATION RESULTS

In this section, simulation results on PAPR and BER are performed to compare the proposed precoded waveform with existing waveforms. The simulation parameters are listed in Table I. For a fair comparison, the same data length and time domain MMSE equalizer are employed for all waveforms.

The CCDF of PAPR of the precoded waveforms are shown in Fig. 2(a), where the curve for the proposed precoder is obtained by averaging 10000 different channel realizations. Under the such configurations, the average l_1-norm of the normalized precoders $\mathbf{U}_{\mathbf{OFDM}}$, $\mathbf{U}_{\mathbf{DFT-s-OFDM}}$, $\mathbf{U}_{\mathbf{OTFS}}$, the adaptive EVD precoder, and the proposed precoder are 8.00, 2.94, 4.66, 7.37, and 2.51 respectively. It can be observed that

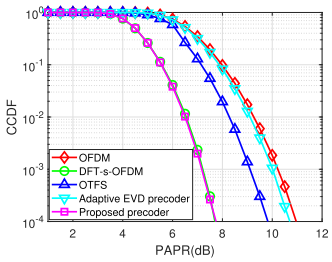

Fig. 2. CCDF of PAPR of the precoded waveforms.

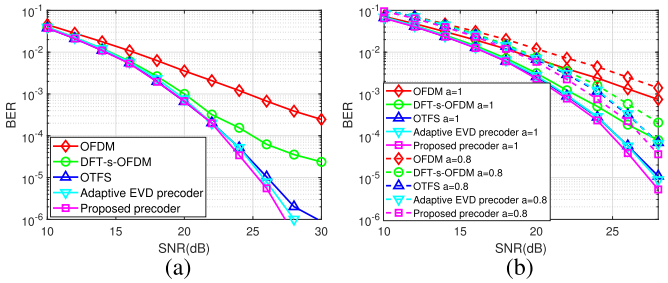

Fig. 3. BER with (a) perfect CSI (b) imperfect CSI.

the PAPR of the proposed precoder is close to DFT-s-OFDM as expected, which is about 2dB lower than that of OTFS, and about 3dB lower than those of OFDM and adaptive EVD precoder. The results validate that the PAPR is effectively reduced by using precoder matrices with lower l_1-norm. With lower PAPR, the proposed waveform is less susceptible to nonlinear distortions and has higher power efficiency.

The BER results of precoded waveforms are shown in Fig.3(a). Due to the lack of compensation for channel impairments at the transmitter, the non-CSI based precoded waveforms show higher BER than CSI based precoded waveforms. OTFS outperforms OFDM and DFT-s-OFDM since it exploits both frequency and time diversity by using the time domain MMSE equalization. It is also observed that the proposed precoder achieves lower BER than existing precoders. That is since the proposed waveform has better resistance to doubly selective fading by maximizing the minimum SINR. The PAPR and BER results indicate that the proposed method has a good potential to handle both nonlinearity and channel fading, and is thus adaptive to more severe scenarios.

To show the effectiveness of our proposed approach in practice, BER under imperfect CSI are also simulated and shown in Fig.3(b). The channel matrix is scaled by a correlation factor a and then added with a Gaussian random matrix ε. The variance of ε is $P_\varepsilon = \frac{\sigma_v^2}{N_p}$, where $N_p = 64$ is the number of pilots. It is observed that the proposed precoder keeps better performance than other existing waveforms. The results verify that the proposed precoder is still competent even with imperfect CSI.

V. Conclusion

In this letter, we have developed a generalized precoded waveform framework based on the TD domain channel response, which can reduce the complexity of the equalizer. Existing waveforms can be generated from our framework. Further, based on knowledge of the channel, a joint precoder and equalizer optimization scheme is proposed to maximize the minimum SINR while holding low PAPR. Simulation results verify that the the proposed precoded waveform achieves better PAPR and BER performance than existing waveforms.

References

[1] T. Jiang and G. Zhu, "Complement block coding for reduction in peak-to-average power ratio of OFDM signals," *IEEE Commun. Mag.*, vol. 43, no. 9, pp. 17–22, Sep. 2005.

[2] D. Qu, L. Li, and T. Jiang, "Invertible subset LDPC code for PAPR reduction in OFDM systems with low complexity," *IEEE Trans. Wireless Commun.*, vol. 13, no. 4, pp. 2204–2213, Apr. 2014.

[3] M. Rajabzadeh and H. Steendam, "Precoding for PAPR reduction in UW-OFDM," *IEEE Commun. Lett.*, vol. 25, no. 7, pp. 2305–2308, Jul. 2021.

[4] A. Mezghani, D. Plabst, L. A. Swindlehurst, I. Fijalkow, and J. A. Nossek, "Sparse linear precoders for mitigating nonlinearities in massive MIMO," in *Proc. IEEE Stat. Signal Process. Workshop (SSP)*, Jul. 2021, pp. 391–395.

[5] Y. Ding, L. Xue, and Z. Wang, "A novel precoding technique to reduce PAPR of UCA-OAM systems," *IEEE Commun. Lett.*, vol. 26, no. 8, pp. 1903–1907, Aug. 2022.

[6] Y. I. Tek and E. Basar, "PAPR reduction precoding for orthogonal time frequency space modulation," in *Proc. 46th Int. Conf. Telecommun. Signal Process. (TSP)*, Prague, Czech Republic, Jul. 2023, pp. 172–176.

[7] Z. Wang and G. B. Giannakis, "Linearly precoded or coded OFDM against wireless channel fades?" in *Proc. 3rd IEEE Workshop Signal Process. Adv. Wireless Commun.*, Taoyuan, Taiwan, Mar. 2001, pp. 267–270.

[8] Y. Ding, T. N. Davidson, Z.-Q. Luo, and K. M. Wong, "Minimum ber block precoders for zero-forcing equalization," *IEEE Trans. Signal Process.*, vol. 51, no. 9, pp. 2410–2423, Sep. 2003.

[9] S. Chan, T. Davidson, and K. Wong, "Asymptotically minimum bit error rate block precoders for minimum mean square error equalization," in *Proc. IEEE Sens. Array Multichannel Signal Process. (SAM)*, Aug. 2002, pp. 140–144.

[10] A. S. Bedi, J. Akhtar, K. Rajawat, and A. K. Jagannatham, "BER-optimized precoders for OFDM systems with insufficient cyclic prefix," *IEEE Commun. Lett.*, vol. 20, no. 2, pp. 280–283, Feb. 2016.

[11] H. Zhang, X. Huang, and J. A. Zhang, "Adaptive transmission with frequency-domain precoding and linear equalization over fast fading channels," *IEEE Trans. Wireless Commun.*, vol. 20, no. 11, pp. 7420–7430, Nov. 2021.

[12] P. Raviteja, Y. Hong, E. Viterbo, and E. Biglieri, "Practical pulse-shaping waveforms for reduced-cyclic-prefix OTFS," *IEEE Trans. Veh. Technol.*, vol. 68, no. 1, pp. 957–961, Jan. 2019.

[13] D. N. C. Tse and P. Viswanath, *Fundamentals of Wireless Communications*. Cambridge, U.K.: Cambridge Univ. Press, 2005.

[14] R. Hadani et al., "Orthogonal time frequency space modulation," in *Proc. IEEE Wireless Commun. Netw. Conf. (WCNC)*, San Francisco, CA, USA, Mar. 2017, pp. 1–6.

[15] A. Jiang, H. K. Kwan, Y. Zhu, X. Liu, N. Xu, and Y. Tang, "Design of sparse FIR filters with joint optimization of sparsity and filter order," *IEEE Trans. Circuits Syst. I, Reg. Papers*, vol. 62, no. 1, pp. 195–204, Jan. 2015.

[16] A. Wiesel, Y. C. Eldar, and S. S. Shamai (Shitz), "Linear precoding via conic optimization for fixed MIMO receivers," *IEEE Trans. Signal Process.*, vol. 54, no. 1, pp. 161–176, Jan. 2006.

[17] Michael Grant and Stephen Boyd. (Sep. 2013). *CVX: MATLAB Software for Disciplined Convex Programming, Version 2.0 Beta*. [Online]. Available: http://cvxr.com/cvx

[18] S. Boyd, S. P. Boyd, and L. Vandenberghe, *Convex Optimization*. Cambridge, U.K.: Cambridge Univ. Press, 2004.

[19] B. Chander Pandey, S. Khan Mohammed, P. Raviteja, Y. Hong, and E. Viterbo, "Low complexity precoding and detection in multi-user massive MIMO OTFS downlink," *IEEE Trans. Veh. Technol.*, vol. 70, no. 5, pp. 4389–4405, May 2021.

[20] *Study Channel Model for Frequencies From 0.5 to 100 GHz*, document TS 38.901, v16.1.0, 3GPP, Dec. 2019.